SKI Report 95:19

Non-destructive Assay of Spent BWR Fuel with High-resolution Gamma-ray Spectroscopy

Ane Håkansson
Anders Bäcklin

May 1995

ISSN 1104-1374
ISRN SKI-R--95/19--SE

SKi
STATENS KÄRNKRAFTINSPEKTION
Swedish Nuclear Power Inspectorate

gotab 13666, Stockholm 1995

SKI Report 95:19

Non-destructive Assay of Spent BWR Fuel with High-resolution Gamma-ray Spectroscopy

Ane Håkansson
Anders Bäcklin

Department of Radiation Sciences, Uppsala University,
Box 535, S-751 21 UPPSALA

May 1995

gotab 13666, Stockholm 1995

1995-03-01

Non-destructive assay of Spent BWR Fuel with High-Resolution Gamma-ray Spectroscopy

Ane Håkansson and Anders Bäcklin
Department of Radiation Sciences, Uppsala University

Abstract

A method, based on high-resolution gamma-ray spectroscopy, has been developed for verification of burnup, cooling time, power history and, to some extent, the initial enrichment of spent BWR fuel. It is shown that, provided that the power history is known and corrected for, burnup and cooling time can be verified with accuracies within 3% and 60 days, respectively, for cooling times up to about 20 years. For cooling times up to about 50 years the corresponding accuracies are 3% and 1.5 years. It is also shown that the above parameters can be determined with no other information than the fuel type. In such cases the accuracies are 3.2% and 170 days, respectively (cooling time <20 years) and 6% and 2 years (cooling time <50 years).

I denna rapport beskrivs en metod baserad på högupplösande gammaspektroskopi att användas för verifiering av utbränningsgrad, avklingningstid och, i viss mån, initial anrikning för BWR bränsle. Förutsatt att korrektion för effekthistorik utförs kan utbränning och avklingningstid med den här beskrivna metoden bestämmas inom 3% respektive 60 dagar för avklingningstider mindre än ca 20 år. För avklingningstider upp till 50 år uppskattas verifieringsnoggrannheten till ca 3% respektive 1.5 år. I rapporten visas också att ovanstående parametrar kan bestämmas utan annan kännedom om bränsleelementen än bränsletyp. Noggrannheten i bestämningen av parametrarna minskas i sådana fall till 3.2% respektive 170 dagar (avklingningstid < 20 år) och 6% respektive 2 år (avklingningstid < 50 år).

1 Introduction

The need of experimental methods for verification or identification of spent nuclear fuel for safeguard purposes is generally recognised. Of immediate interest are methods to verify that nuclear power plants have been operated as stated by their operators and that the spent fuel with its contents of fissile material has not been manipulated during its transportation or storage. Later, at the end of the fuel cycle, the fuel will be permanently encapsulated and placed in the final repository. Safeguard reasons will then demand a high degree of assurance that the nuclear material encapsulated is in accordance with the book-keeping.

Non-destructive assay of spent nuclear fuel can be made by measuring the radiation emitted, either neutrons or gamma-rays. High-Resolution Gamma-Ray Spectroscopy (HRGS) is a potentially useful method for verification and identification of spent fuel. It is based on measurements of the concentration of the fission products ^{137}Cs, ^{134}Cs and ^{154}Eu. Advantages with this method are: (i) Two or more isotopes with different gamma-ray energies are measured, which give information on different fuel parameters (see below). (ii) The relationship between the concentration of ^{137}Cs and the burnup of the fuel is very nearly linear. (iii) The measurement is passive, i. e. no external radiation source is needed. (iv) The primary data registered are spectroscopic in character, implying that the quality of the measurement can easily be checked by inspecting a computer screen. This may be used to identify and eliminate problems that may arise from disturbing electric fields or other malfunctions.

The HRGS method has been discussed earlier, see e. g. ref. /1 - 4/. It has been studied and further developed in Sweden during several years in a co-operation between the Department of Radiation Sciences at Uppsala University and the Swedish Nuclear Power Inspectorate (SKI). In the present report we describe the equipment developed for the work, the methods for analysing the data and some results obtained. Parts of this work has been reported earlier, ref. /5 - 8/.

2 The HRGS method for BWR fuel.

2.1 Basic fuel parameters.

In spent nuclear fuel the concentration of fission products at a given moment depends on a number of quantities or circumstances, in the following called fuel parameters, which are characteristic for an individual fuel assembly. The most important fuel parameters in the present context are:

Burnup (BU)
Cooling time (CT)
Initial enrichment
Power history
Integrity

The parameters represent averages over the whole fuel assembly. The parameter "integrity" is introduced in order to account for the fact that assemblies sometimes have been reconstructed in such a way that the original rods have been replaced or, sometimes, removed.

Of the five parameters listed, BU and CT are by far the most important for the concentrations of the fission products. By measuring the gamma-ray intensities from two fission products, these two quantities can be determined to first order since the fission products all have different half-lives.

The three remaining fuel parameters have less influence on the concentrations of the fission products. The power history has an observable influence on the intensities measured, implying that this parameter to some extent can be verified in the measurements. In practice this is done by using the operator declared values for the relevant parameters for calculating corrections to the values of BU and CT obtained in first order. If the measurements are accurate enough significant deviations

between the corrected experimental values of BU and CT and the operator's declared values will then result if the actual power history deviates from the declared one.

The influence of the two remaining fuel parameters, the original enrichment and the integrity, have not been studied in detail here. Calculations with the code ORIGEN 2, ref. /9/, indicate that the yields of ^{134}Cs and ^{154}Eu depend somewhat on the initial enrichment. Our data suggest that this parameter only has a minor influence on the gamma-ray intensities measured here. We have accordingly attempted a simplified procedure of correction for the influence of this parameter as presented in section 2.6. A more detailed treatment is, however, required in order to conclude to what degree of accuracy the initial enrichment can be determined with the HRGS method

The present set of data definitely indicate that the gamma-ray intensities are sensitive to the integrity of the fuel assemblies. It has however not been possible here to make a quantitative study of this effect.

2.2 Principle of the experiment.

The concentration of ^{137}Cs depends almost linearly on BU. In a typical Swedish BWR fuel the deviation from linearity for BU below 40 GWd/tU is less than 0.2% as calculated with the code ORIGEN 2, ref. /9/. For ^{134}Cs and ^{154}Eu the relation between the concentration and BU is more complex, see figs. 2.1 and 2.2.

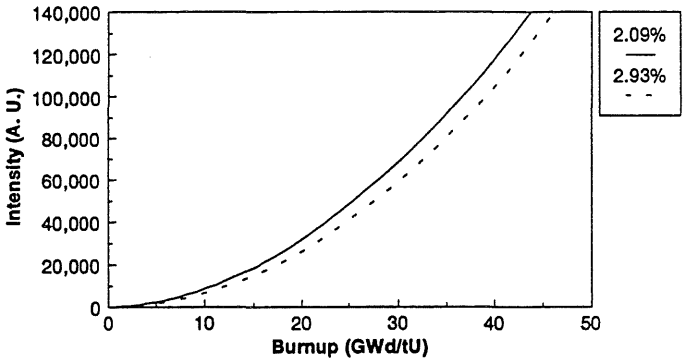

Figure 2.1. The ^{134}Cs intensity as calculated with ORIGEN 2 for two different initial enrichment v. s. burnup.

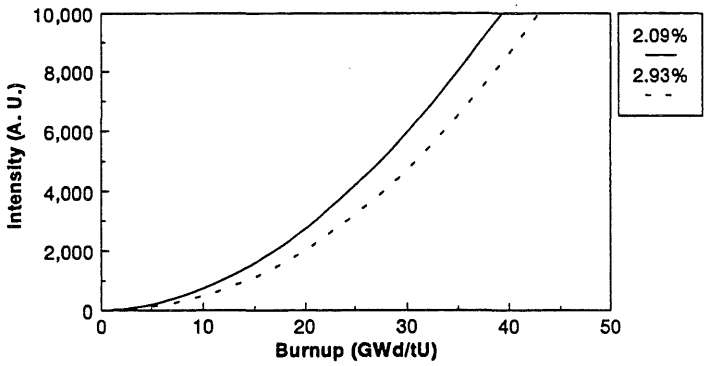

Figure 2.2. Same as in fig. 2.1 but calculated for ^{154}Eu.

Due to its mode of production the concentration of ^{134}Cs depends essentially quadratically on the BU. The BU dependence of the concentration of ^{154}Eu is much more complex due to the fact that it is produced via many different mass chains of which five have a major importance, cf. fig. 2.3. The resulting yield curve, however, agrees decently well with a quadratic curve up to values of BU of about 40 GWd/tU, fig. 2.2.

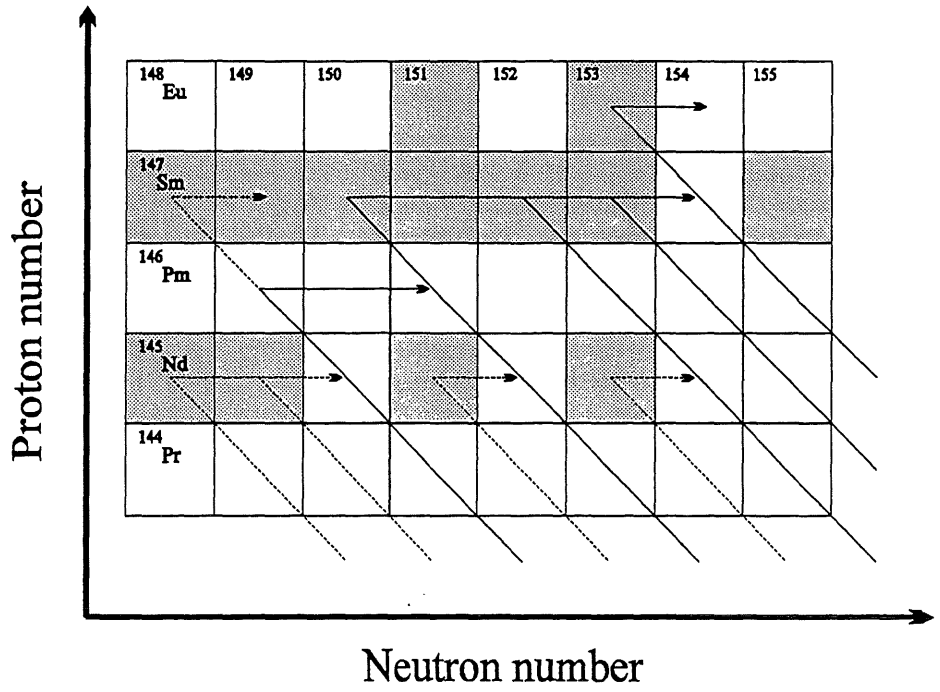

Figure 2.3. The main mass chains which contribute to the production of ^{154}Eu.

The experimental arrangement is shown schematically in fig. 2.4. The fuel assembly is mounted in an elevator on the inside wall of a fuel handling pool. Gamma radiation from the assembly passes

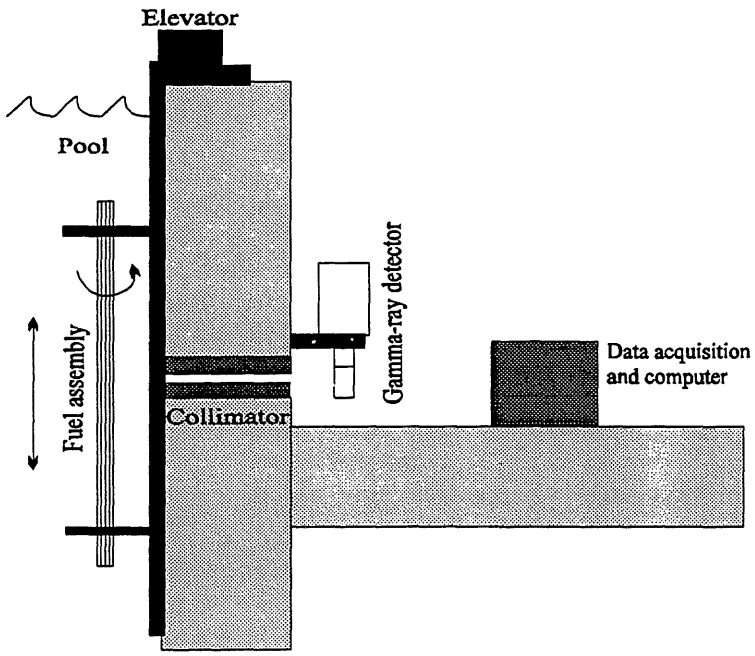

Figure 2.4. The experimental arrangement.

through a horizontal slit in a collimator in the pool wall, which allows the detector outside the wall to see a part of the assembly with a height of a few mm and a width equal to the diagonal of the quadratic fuel assembly.

The average gamma-ray intensity from the assembly is obtained by moving the full length of the assembly across the slit position while measuring the intensity of the radiation. Due to the rather large radial gradient of the BU of a BWR assembly, which generally is of the order of 10% between the corners, the measurement is repeated four times, once for each corner of the assembly facing the detector, and the final intensity is obtained as the sum of these measurements.

These summed gamma-ray intensities are assumed, in a first approximation, to be directly proportional to the corresponding average concentrations of fission products and thus to depend in the same way as the latter on the fuel parameters listed above. The gamma-ray intensities also depend on general circumstances such as the experimental geometry used and the specific type of assembly measured. This is taken into account by a calibration procedure, in which a number of fuel assemblies for which the BU is considered to be known, are measured.

Due to the self-absorption within the assembly, the measured intensities depend slightly on the internal structure of the assembly, i. e. how the fuel rods with different enrichment are distributed in the assembly. The latter effect has to be corrected for by calculations based on information of this distribution.

2.3 Determination of the burnup

From the measured average gamma-ray intensity of ^{137}Cs , the burnup can be calculated from the expression:

$$I_1 = K_1 \beta e^{-\lambda_1 cT} \alpha_1^{-1} \qquad \text{(Eq. 2.1)}$$

Here I_1 and λ_1 are the intensity and the decay constant for ^{137}Cs, respectively. The burnup is denoted with β and α_1 is the correction factor for irradiation history. The coefficient K_1 is a product of two factors A and B where A depends only on the geometry of the measured fuel assembly and B depends only on the geometry of the detector and collimator arrangement. The factor B is in turn a product of four factors determined by:

i) the effective area of the assembly as seen from the detector.
ii) the transmission of the radiation through the absorbing media between the fuel and the detector.
iii) the solid angle covered by the part of the detector that can be seen through the collimator by the assembly.
iv) the intrinsic efficiency of the detector 662 keV radiation, i. e. the probability that a quantum hitting the detector will result in the storing of an event in the full energy absorption peak in the spectrum.

The burnup of an assembly can be experimentally obtained from a gamma-ray measurement provided that the proportionality constant K_1 has been determined. Such a calibration should be carried out with great care, using as large a set of fuel assemblies as possible and least squares fitting eq. (2.1) to the data. It is clear from above that such a calibration only holds for i) the same type of fuel assembly as that to be measured and ii) using identically the same experimental geometry. The first of these two requirements is unconditional. The second requirement can be difficult to realise since the experimental conditions may change from occasion to occasion. This can be handled by measuring a reference fuel assembly at each occasion of measurement, dividing the value of K_1 obtained with the value obtained for that particular assembly in the earlier calibration measurement, and using the ratio for correcting the count rates obtained. An other way to provide proper calibration is to use a reference source, see section 3.4.

The expression corresponding to eq. (2.1) for the ^{134}Cs and ^{154}Eu-intensities can be written as:

$$I_2 = K_2 \beta^{\kappa} e^{-\lambda_2 cT} \alpha_2^{-1} \qquad \text{(Eq. 2.2)}$$

Here κ is an exponent, close to 2, that is determined in a fitting procedure. The other parameters have a meaning analogous to those in eq. (2.1).

If two activities are measured, BU and CT can be obtained by combining eqs. (2.1) and (2.2). Solving for β gives:

$$\beta = \left(\frac{\alpha_2 I_2}{K_2} \left(\frac{K_1}{\alpha_1 I_1} \right)^{\frac{\lambda_2}{\lambda_1}} \right)^{\left(\kappa - \frac{\lambda_2}{\lambda_1}\right)^{-1}} \qquad \text{(Eq. 2.3)}$$

The coefficients of the propagation of the errors of the measured gamma-ray intensities are inversely proportional to the decay constants. This is fortunate since the accuracy is highest for the intensity of the long-lived ^{137}Cs. It is also fortunate that the inequality $\lambda_2/\lambda_1 \neq \kappa$ holds here since the exponent in eq. (2.3) otherwise would be infinite.

A condition for the calculation of the burnup is that the correction factors α_j for power history can be calculated. This is only possible if the operator can provide relevant information on the power history. If this information is lacking the burnup can still be determined but with somewhat less accuracy, see section 5.

2.4 Determination of the cooling time

The cooling time can be calculated by combining eqs. (2.1) and (2.2) and solving for CT. This results in the following expression:

$$CT = \frac{1}{\lambda_2 - \kappa\lambda_1} \ln\left\{ \left(\frac{\alpha_1 I_1}{K_1} \right)^{\kappa} \frac{K_2}{\alpha_2 I_2} \right\} \qquad \text{(Eq. 2.4)}$$

The accuracy in the determination of cooling time increases with the ratio λ_2/λ_1, which favours the use of ^{134}Cs and ^{137}Cs. However, the comparatively short half-life of ^{134}Cs makes it too weak to be measured at cooling times longer that about 20 years. For longer cooling times it is therefore necessary to use ^{154}Eu together with ^{137}Cs.

Regarding the power history correction factors α_j, the same reservations are valid here as for the burnup calculations. If these factors are not introduced the errors in the calculated cooling time increase significantly, cf. section 5.

An alternative way of determining the CT for periods less than about 20 years is to use the intensity ratio $^{154}Eu/^{134}Cs$. If the exponent κ and the correction factors α_j in eq. (2.2) are assumed to be equal for ^{134}Cs and ^{154}Eu, which are fair approximations, the CT can be determined directly from the intensity ratio without further information than the values of the calibration constants K_2 and K_3 from

$$\frac{I_2}{I_3} = \frac{K_2}{K_3} e^{-(\lambda_2 - \lambda_3)CT} \qquad \text{(Eq. 2.5)}$$

Here index 2 and 3 indicate ^{154}Eu and ^{134}Cs, respectively.

2.5 The Power history.

The reactors considered here are generally operated in power cycles lasting about one year including a shut-down period of 1-2 months. Figure 2.5 shows schematically the yield curve of a fission product assumed to grow linearly with the BU. The yield of the isotope at the end of the final irradiation period depends, besides on the BU and the half-life of the isotope, on the number of power cycles during which the BU was acquired, and the detailed power profile of each cycle. Therefore, in order to make possible to compare on the same scale the concentrations of fission products in assemblies with different power histories, the measured gamma-ray intensities must be adequately corrected. In the present case the half-lives of the three isotopes studied are long enough to allow neglecting the detailed power distribution during a cycle. The correction is therefore limited to considers only the number of power cycles and the burnup added in each cycle as declared by the operator.

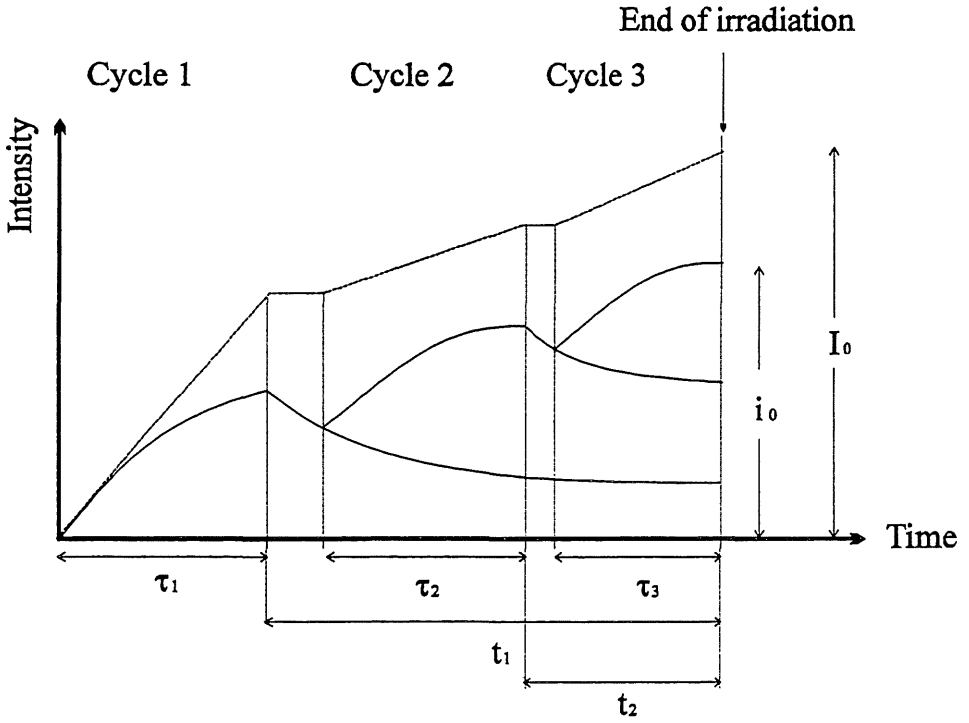

Figure 2.5. Production of a direct fission product without (dashed line) and with (full line) decay taken into account. A correction factor α is formed by the ratio I_0/i_0.

Figure 2.5 suggests a correction factor α for irradiation history as the ratio between the two cases shown in the figure. The intensity I_0 in figure 2.5 can be calculated from operator declared data for each power cycle according to:

$$I_0 = K_1 \sum \beta_n \qquad \text{(Eq. 2.6)}$$

Where β_n is the burnup acquired in cycle n.

For calculating i_0 in figure 2.5 the following differential equation holds:

$$\frac{di}{dt} = K_1 p - \lambda i \qquad \text{(Eq. 2.7)}$$

Here p is the power produced during each power cycle. In this treatment we assume p to be constant. The general solution of eq. (2.7) is:

$$i = \frac{K_1 p}{\lambda}(1 - e^{-\lambda t}) \qquad \text{(Eq. 2.8)}$$

During each power cycle n, the fuel is irradiated for a period of time of τ_n producing the gamma intensity i_n. The yield i_0 , which is i_n summed over all power cycles, can thus be described as:

$$i_0 = K_1 \sum \frac{\beta_n}{\lambda \tau_n}(1 - e^{-\lambda \tau_n}) \qquad \text{(Eq. 2.9)}$$

In this expression we define $\beta_n = p\tau_n$. To take into account the decay of the fission product during the period from the end of cycle n to the end of the last cycle, i_n has to be multiplied by a factor $e^{-\lambda t_n}$, where t_n is the period of time from the end of the n:th cycle to the end of the last cycle.

From eqs. (2.6) and (2.9) α is calculated as:

$$\alpha = \frac{\sum_{n=1} \beta_n}{\sum_{n=1} \frac{\beta_n}{\lambda \tau_n}(1 - e^{-\lambda \tau_n})e^{-\lambda t_n}} \qquad \text{(Eq. 2.10)}$$

For ^{134}Cs and ^{154}Eu, where the intensity does not follow a linear relationship with burnup, the treatment in principle becomes more complicated. However, by making some approximations one may obtain simple expressions which still provide sufficient accuracy. Assume that the intensity I_0 depends on burnup as in eq. (2.11).

$$I_0 = K_2 \beta^{\kappa} \qquad \text{(Eq. 2.11)}$$

The intensity contribution Δi_n for each cycle can now be calculated according to:

$$\Delta i_n = K_2(\beta_n^{\kappa} - \beta_{n-1}^{\kappa}) \qquad \text{(Eq. 2.12)}$$

Here K_2 is a constant and β_n is the actual burnup at the end of cycle n. In this equation we make the assumption that all power cycles have the same duration, which is a good approximation in the assemblies studied in this report. When this assumption does not hold a more elaborate treatment is necessary in which the decay of the fission products during irradiation is taken into account.

By summing Δi_n over all cycles we obtain the total intensity i_0 as:

$$i_0 = K_2 \sum(\beta_n^{\kappa} - \beta_{n-1}^{\kappa}) \qquad \text{(Eq. 2.13)}$$

The ratio between eqs. (2.11) and (2.13) gives α as:

$$\alpha = \frac{\beta^{\kappa}}{\sum(\beta_n^{\kappa} - \beta_{n-1}^{\kappa})e^{-\lambda t_n}} \qquad \text{(Eq. 2.14)}$$

Note that α depends on the relative burnup rather than the absolute burnup at the end of cycle n.

The correction factor for ^{137}Cs as calculated from eq. (2.10) for two typical cases of power history is given in table 2.1. For ^{134}Cs and ^{154}Eu eq. (2.14) must be applied. The variations in the correction factors given in table 2.1 are seen to be much larger than for ^{137}Cs, which is due to the comparatively much shorter half-lives in these cases. This relatively strong dependence of the measured gamma-ray intensities on the power history can in principle be used to verify that the power history of the fuel assembly measured is in agreement with the operators declaration.

Isotope	*5 cycles*	*7 cycles*
^{137}Cs	1.0624	1.0885
^{134}Cs	1.4269	1.6835
^{154}Eu	1.1098	1.1722

Table 2.1. Correction factors for the three isotopes considered here, calculated for two typical power histories. The factors are independent of the BU. In calculating the values for ^{134}Cs and ^{154}Eu, κ was set to 2 for simplicity.

2.6 The initial enrichment

In principle the initial enrichment of the fuel influences the yields of all fission products to a degree that depends on at first hand the burnup. To investigate this effect calculations were made with ORIGEN 2, ref. /9/ for a number of BWR assemblies with different enrichment, burnup and power history. The effect for ^{137}Cs was found to be too small to be of interest here but for ^{134}Cs and ^{154}Eu the relative yields may vary of the order of 10% per percent enrichment for homogeneous fuel cf. figs. 2.1 and 2.2. In the fuel investigated here, the fuel pins with the highest enrichment are concentrated to the centre of the assembly which, in view of the self-absorption of the gamma radiation in the assembly, can be expected to reduce the effect of the variation of the enrichment. An detailed calculation of the total effect is rather complex because it involves a combination of burnup calculations for individual fuel pins, isotope yield calculations and self-absorption calculations.

Since the assemblies investigated here do not differ much with respect to the enrichment of the fuel, a simpler, very approximate approach was adopted. The yields for ^{134}Cs and ^{154}Eu were calculated for each of the initial enrichment considered in this investigation, using ORIGEN 2. From these calculations a correction factor:

$$C_i = 1 + f\frac{y_{3.0} - y_i}{y_i} \qquad \text{(Eq. 2.15)}$$

was formed where y_i is the calculated yield for the average enrichment and burnup of the i:th assembly, $y_{3.0}$ is the yield for fuel with the enrichment 3.0%, which is used as a reference value and the same burnup as used in y_i,. An adjustable factor f is introduced in order to optimise the effect of C_i. The calculations were made for different cases of power history which, however, showed no difference in the resulting values of C_i. The correction for enrichment was made by applying the correction factors C_i to the intensities of ^{134}Cs and ^{154}Eu and, using the complete set of data, fitting the factor f together with the parameters K_2 and κ to obtain the best fit to eq. (2.2). The best fit was obtained for f=-0.1 in ^{134}Cs and f=0.3 for ^{154}Eu, cf. fig. 2.6. In comparison with the case with no correction for enrichment, corresponding to f=0, the relative S. D. of the fits were changed from 4.6% to 4.5% in the ^{134}Cs case and from 6.1% to 6.0% in the ^{154}Eu case. The effect was more pronounced for some of the subsets of data discussed in section 5.

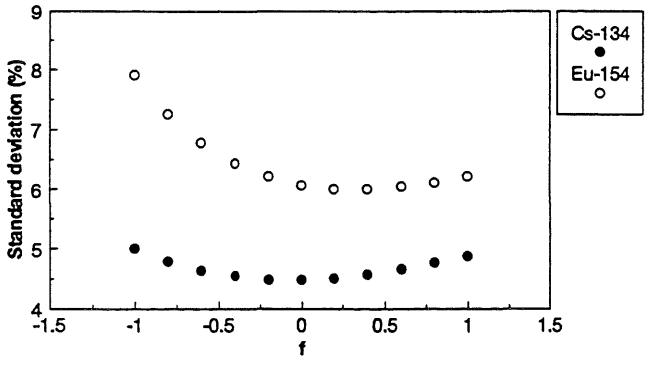

Figure 2.6. Standard deviations of individual points for the fit of ^{134}Cs and ^{154}Eu as a function of the parameter f. A minimum is obtained at f=-0.1 for ^{134}Cs and f=0.3 for ^{154}Eu.

2.7 Correction for fuel pin configuration

The gamma absorption coefficient of UO_2 of about 1.16 cm^{-1} for 662 keV gamma energy implies that radiation from fuel pins with different radial positions in an assembly contributes differently to the total radiation emitted as discussed in section 2.6. The fuel assemblies are in general designed with a radial distribution with respect to initial enrichment in order to compensate for radial differences in the thermal neutron flux. This implies that the radial distribution of the burnup will not be constant, but will in general have a gradient that may change with time. However, the radial burnup distribution tends to level out as the burnup increases.

In order to investigate the influence of these effects on the gamma-ray intensities, a two-step calculation was made. First the burnup of each fuel pin in a fuel assembly was calculated for a number of values of the total burnup of the assembly using the CASMO2,3* code. In the second step these burnup values were introduced in the code CHICHA, which calculates the total gamma-ray intensity emitted from the fuel assembly considering the self absorption in the fuel assembly and absorption in the surrounding water.

The calculations were limited to ^{137}Cs; for the other two isotopes the calculations are more complex. Figure 2.7 shows ratios of such calculations with three typical but different configurations corresponding to initial enrichment of 3.03%, 2.82% and 2.06% as a function of the burnup. It is seen that the ratios only slightly deviate from the value 1.00, especially for burnup values larger than 25 GWd/tU which is the region of interest in this report. Considering that the inaccuracies due to other effects generally were observed to be of the order of several percent, the experimental data were generally treated without considering this effect.

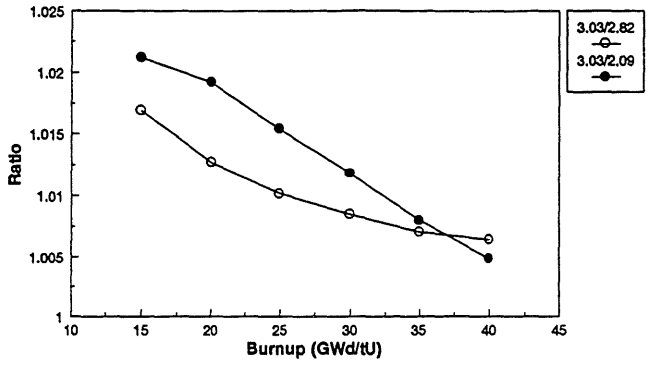

Figure 2.7. Ratios between gamma intensities calculated with the code CHICHA for three fuel assemblies with different fuel pin configuration as a function of burnup. This figure illustrates that the correction for this effect is relatively small.

3 Experimental equipment

3.1 The mechanical arrangement

The mechanical arrangement of the fuel assembly and the collimator is shown in figure 2.4. Such installations are present in all Swedish BWR plants and at the storage plant CLAB at Oskarshamn, where most of the measurements reported here have been performed.

The fuel assembly to be measured is mounted in a fixture in the elevator with a precision of the positioning of about ±1 mm in the lateral dimensions. The fixture can azimuthically be rotated 360° manually or with the aid of a stepping motor with a precision of about 0.2°.

The elevator system used to move the fuel assembly vertically has an adjustable speed control which is used to optimise the speed with respect to fuel length, scanning time etc. At the same setting of the control, the speed in the downward direction is about 20% faster than in the upward direction due to the action of gravity. However, the speed in both directions have been found to be constant within less than 1% during scans.

When mounted in the fixture the distance between the centre of the fuel assembly and the pool wall is about 50 cm.. The transmission of gamma radiation through the water is about 1% for 662 keV and 3% for 1275 keV (^{154}Eu).

The collimator arrangement consists of two massive, 200 mm in diameter steel half-cylinders which sandwich a thin steel plate. The collimator height is defined by a slit routed in the steel plate. The design is such that the slit width is 50 mm at the detector end and increases at the fuel end so that the

* The authors are grateful to Ewa Kurcyusz at Vattenfall Fuel AB for assisting in these matters and performing the CASMO calculations.

full fuel width can be viewed by the detector. With this arrangement the slit height can be changed from 1 mm to 5 mm by interchanging slit plates. The total weight of the collimator is about 200 kg. All surfaces which defines the slit is machined to a precision of about 20 μm. The length of the collimator is 120 cm and the detector is located 175 cm from the centre of the fuel assemblies.

3.2 The detector system

The requirement to detect the radiation from different isotopes separately necessitates the use of a high-resolution gamma-ray spectroscopy system based on a germanium detector. The system should be able to measure fuel with a cooling time of several decades, when the activities of ^{134}Cs and ^{154}Eu are very weak. To measure these weak intensities in the presence of the strong intensity from ^{137}Cs the specifications of the system should be maximised with respect to two parameters:

i) The ratio between the peak area and the corresponding Compton area in the spectrum should be as high as possible. This generally implies the use of as large a detector as possible. Due to economical reasons the size of the detector was limited to 40% relative efficiency.

ii) The system should be able to operate efficiently at as high count rates as possible. Generally, high count rate can not be obtained simultaneously with the highest energy resolution. In the present case a high count rate is strongly preferred since the line density in the spectra is generally rather low, implying that wide energy regions around the peaks are available to define the background with good statistics. A schematic lay-out of the detector system, is shown in figure 3.1.

The detector is irradiated radially, since it was observed that in this geometry the peak area was less sensitive to count rate variations than in a geometry with axial irradiation, ref. /10/. In general a filter of 4 or 8 mm lead is used for filtering of the otherwise strong low-energy distribution of scattered radiation.

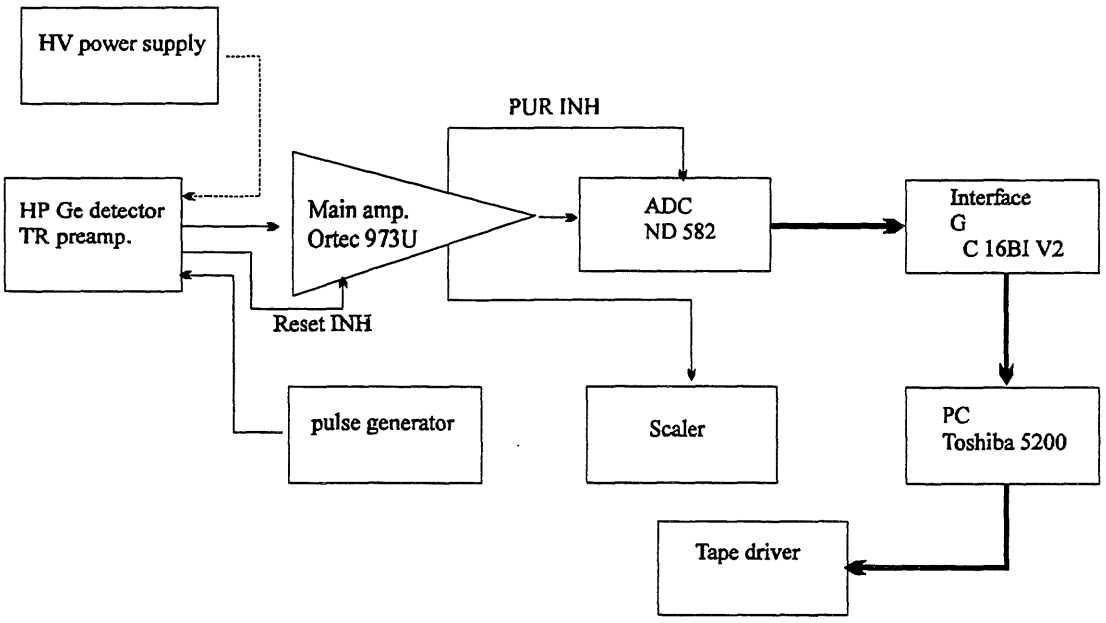

Figure 3.1. Schematic view of the detector system used.

The pulses are processed by a transistor reset pre-amplifier and a gated integrator amplifier type Ortec 973 U with 1.5 μs or 3.0 μs integration time. The ADC is of the type ND 582 with a fixed nominal conversion time of 1.5 μs (2.4 μs with read-out). The digitised pulses are stored in the RAM of a PC via a fast interface card that was especially developed for the purpose. With a comparatively fast PC the throughput curves shown in figure 3.2 were obtained.

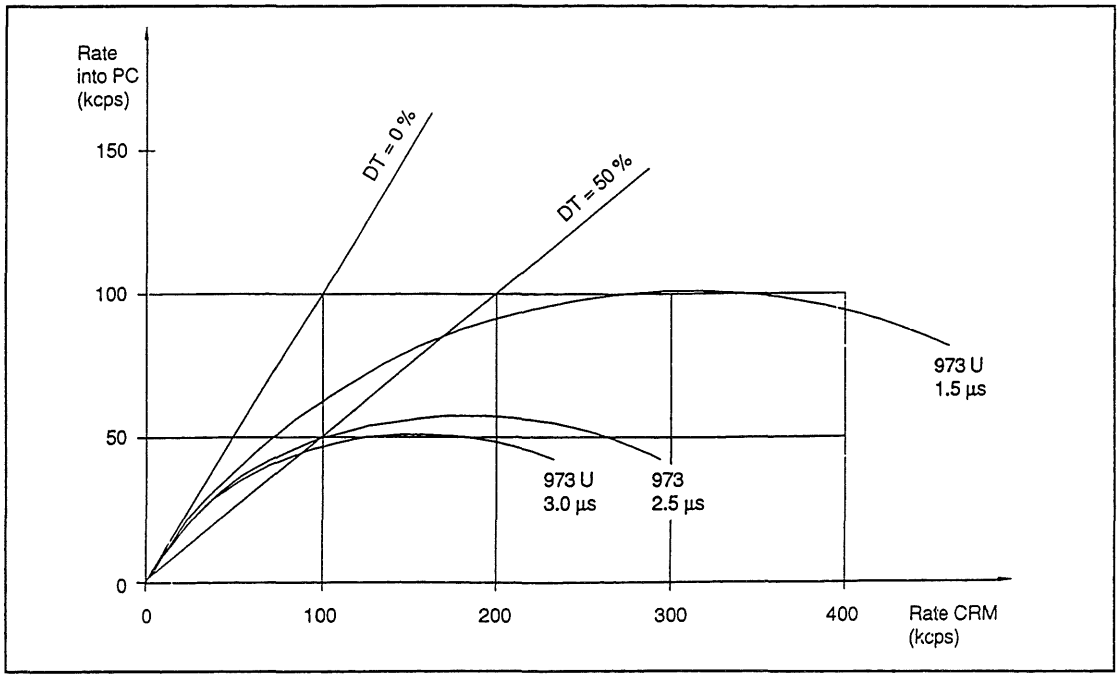

Figure 3.2. Throughput curves obtained for the present detector system.

The energy resolution agrees decently with the values indicated by the manufacturer of the amplifier system, i. e. typically 2.5 keV FWHM at 1332 keV using the 3 µs integration time option and 3.0 keV using the 1.5 µs integration time.

At the high count rates used, often corresponding to more than 50% dead-time, it is important to make an adequate correction for the total dead-time in the system. For this purpose the pulser-method has been employed as indicated in figure 3.3 which shows a typical energy spectrum. The pulser rate is normally adjusted to 2 kHz and the amplitude is adjusted so that the peak lies alone in the high-energy part of the spectrum.

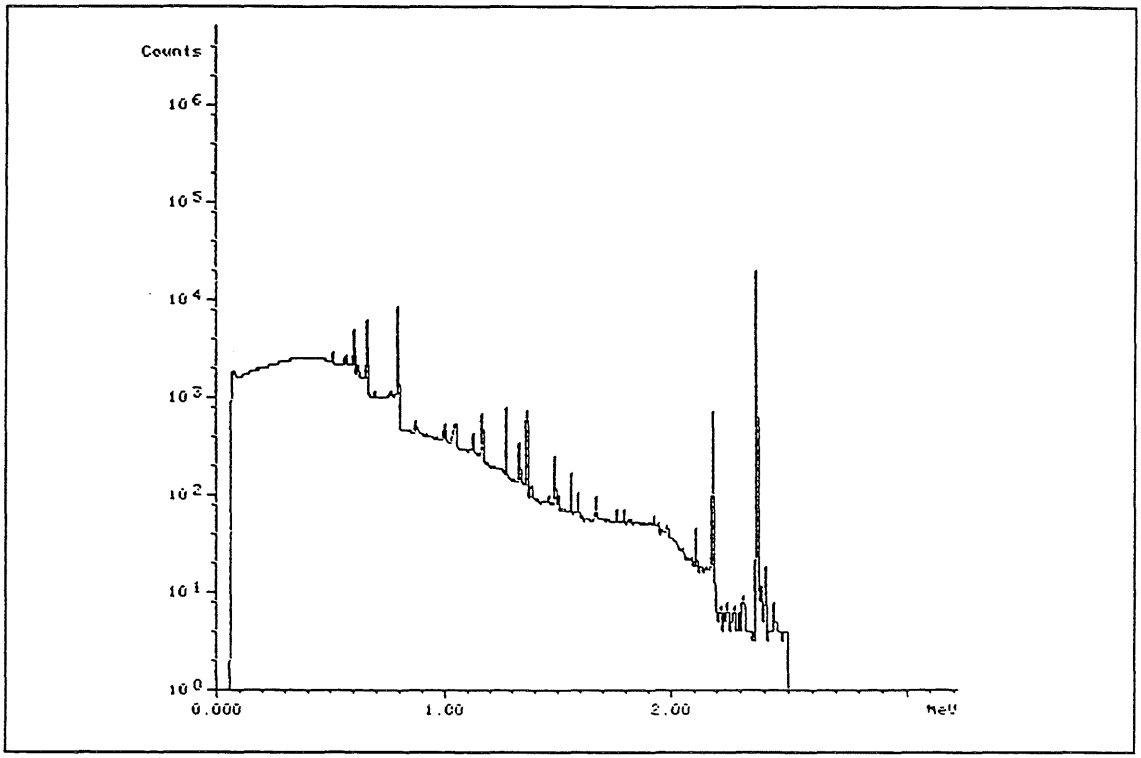

Figure 3.3. Energy spectrum obtained with the detector system. The spectrum is recorded from a fuel assembly with BU=40.4 GWd/tU and CT=672 days.

3.3 Software

A special software package SEDAS containing a data acquisition module and an analysis module was designed for data acquisition and subsequent analysis of data. A flow chart of the main parts of the package is shown in figure 3.4.

The data acquisition module essentially performs "multi spectrum scaling", i. e. it continuously stores data from the ADC while switching the data area with regular time intervals T. The switching is performed in less than a micro second, so essentially no data are lost in the process. Three data areas are employed in cyclic permutation. During the first cycle data are stored in area #1. During the second cycle the data acquisition is directed to area #2 while the data in area #1 are transferred to the hard disc. The procedure is repeated for area #3 and area #2, respectively, during the third cycle, while the contents in area #1 is reset. When the data acquisition is finished, i. e. when spectrum #N has been stored, the sum of all spectra is displayed in spectrum area #4.

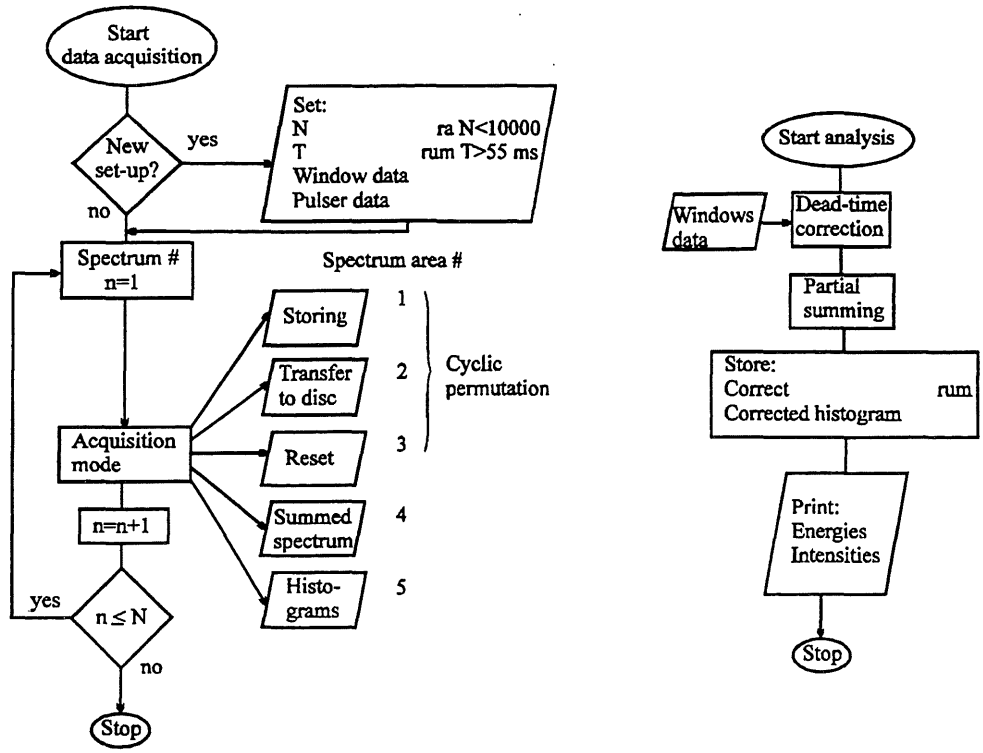

Figure 3.4. Flow chart of the software part of the data acquisition system used for the measurements and analysis.

Before the acquisition is started the cycle time T and the number of intervals N have to be decided. Also information on the pulser frequency and the position of the pulser peak in the spectrum have to be given as input to the subsequent dead time correction procedure. The values of N and T should be chosen so that the product NT corresponds to the scan time of the fuel. For example, if the fuel length to be scanned is 5 m, the spatial resolution required is 1 cm and the scan time wanted is 120 s, the values of N and T are 500 and 0.24 s, respectively. For reasons of simplicity of the software, the adjustment of T can only be made in steps of 55 ms, which makes the scan time 110 s for fuel moving downwards and 137 s for fuel moving upwards if the spatial resolution should be exactly 1.00 cm. In principle there is no upper limit for N, except for the size of the hard disc used.

If the operator wants to follow the process of the data acquisition during a scan of the fuel, the net count rate in a number of peaks or other energy intervals can be monitored and displayed during the scan, provided that the energy window information has been given in the set-up procedure. The windows information needed for each peak is upper and lower limits of the regions defining the peak and the background on each side of the peak.

The net intensity of each peak is shown as a histogram displayed in spectrum area #5. An example of such histograms is shown in figure 3.5.

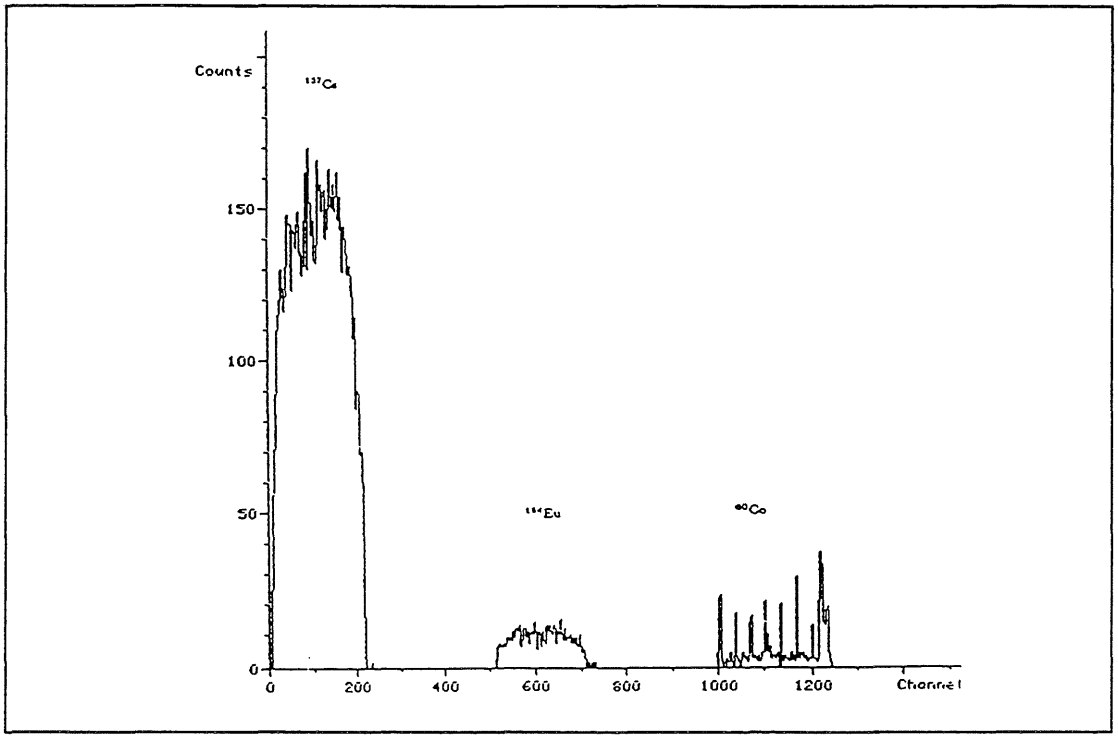

Figure 3.5. Examples of intensity distributions for ^{137}Cs, ^{154}Eu and ^{60}Co as recorded by the software package SEDAS. In this figure, N=250 spectra and T was 0.88 s. Note the concentration of ^{60}Co in the supporting structure, especially the rod holders.

The acquisition procedure as described above relies on the assumption that the relation between the axial position of the fuel assembly and time during a scan is linear with a sufficient accuracy. If this is not the case, i. e. if the vertical movement of the assembly is irregular, the equipment must be complemented with a position indicator. Provisions are taken in the hardware and software for counting of pulses from a positioning device and correcting the spectra accordingly.

After the scan is finished the data collected are corrected for dead-time and evaluated by the analysis module. This can be started automatically or manually. The input is a window information table and the file with N spectra obtained in the data acquisition. The analysis module corrects each of the N spectra for dead-time and creates a summed dead-time corrected spectrum and dead-time corrected histograms of the selected peaks.

The final section of the analysis module contains a routine for normalising the histograms so that each bin corresponds to the same part of the fuel assemblies independently of the direction of the movement of the assembly during recording, a routine for correcting the histograms for variations in the speed of the assembly and a routine for summing over partitions of the histograms. These partitions are usually made the same as those defined as nodes in the operator's core physics calculations. Generally 25 evenly distributed nodes are used. Routines are also available for additional calculations such as summing over a selected number of nodes, summing over the four corners etc. Figure 3.6 shows the nodal distribution of the intensity from ^{137}Cs summed over all corners compared with the corresponding core physics calculations.

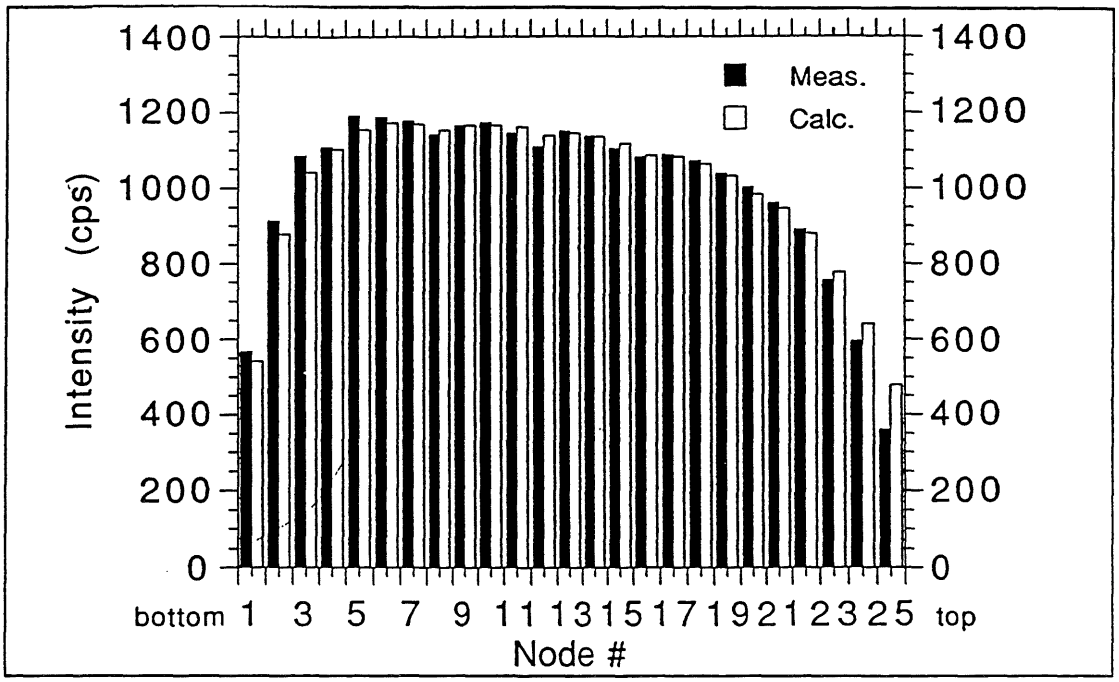

Figure 3.6. Experimental ^{137}Cs intensity distribution together with a burnup distribution based on the operator core physics calculation. The mean values for each distribution have been used to normalise the experimental values to the calculated ones

3.4 Reference source

The results that can be obtained with the equipment described above are all based on a local calibration of the equipment, i. e. the value measured for K_1 in eq. (2.1) is only valid in the particular experimental configuration used. In order to increase the usefulness and reliability of the results it would be valuable to be able to compare them with similar measurements obtained at other sites. This would be possible if the same assembly could be measured at different sites as discussed in section 2.3. To avoid the impractical and expensive transportation needed in such a procedure a more easily transportable reference source has been assembled, ref. /2/. It consists of a point source of about 1 Ci ^{137}Cs fitted into a standard BWR fuel channel, which can be placed in the same fixture as the fuel assemblies to be measured. To simulate a vertically extended source, the ^{137}Cs pellet is oscillated vertically with a constant velocity. The source need not to be extended horizontally provided that the width of the collimator slit used is constant within an accuracy of about 1%. A further discussion is found in ref. /6/.

4 Measurements

The results reported in this paper is based on data from three measuring campaigns labelled F, G, I. The measurements took place at two different sites. Campaign F was performed at the F2 reactor at the Forsmark nuclear power plant the two other were performed at CLAB. The assemblies studied at CLAB were delivered from Forsmark 2, Barsebäck 1, Oskarshamn 3 and Ringhals 1.

The measurements were concentrated on BWR assemblies of the ABB Atom 8×8 type, but a few (5) assemblies of the type SVEA 64 were also measured at Forsmark 2. In total 52 BWR assemblies of the 8×8 type were measured. Of these 44 were characterised as regular, i. e. they had not been reconstructed by changing any fuel pins between the irradiation periods. In addition, 8 assemblies declared as reconstructed were measured. These assemblies are omitted in the following discussion since they are (i) too few to permit definite conclusions and (ii) not selected in a systematical way. The latter remark is due to the fact that these assemblies in a first instance were declared as regular ones. There are, however, indications that the results from the reconstructed assemblies as well as the

SVEA 64 fuel deviate slightly from the ordinary 8×8 type fuel. In the following the results and the discussion is focused on the regular 8×8 type assemblies.

Each assembly was scanned four times, once for each corner facing the detector. The number of spectra N was generally set in the range 150 to 250, corresponding to an axial resolution in the range 3.0 cm to 1.8 cm. The measuring time was typically around 1.0 s and 1.5 s per spectrum for the downward and upward movement, respectively. The collimator slit widths were 3 mm at Forsmark and 5 mm at CLAB. The detector was firmly attached to the pool wall in all measurements, since a slight translation of the detector can affect the efficiency of the detector.

With fuel in the range 20<BU<40 GWd/tU and 2<CT<8 years, total count rates in the range 20 kHz to 50 kHz were obtained. Typically the total number of counts collected in the ^{137}Cs peak for an assembly was in the range $3 \cdot 10^5$-10^6, all four corners added. For the 1275 keV peak in ^{154}Eu, the intensity was typically a factor of 10-20 weaker. With these count rates the integration time constant of 3.0 us in the main amplifier could generally be used with dead-times in the range 20% to 50% and an energy resolution in the range 2.3-2.6 keV for the ^{60}Co peaks. The energy range of the spectrum was in general about 3 MeV in order to include the 2.18 MeV gamma line from ^{144}Pr. The pulser peak was always located at the high energy region of the spectra, approximately at 2.8 MeV, where the influence of the background radiation was negligible.

5 Results

5.1 Procedure of evaluation and presentation

For each campaign the measured gamma-ray intensities of the 661 keV line in ^{137}Cs and the 5-6 strongest lines in ^{134}Cs and ^{154}Eu were evaluated and summed over the four corners for each node as described in section 3.3. In the following, results are presented for the strongest line in each isotope, i. e. the 661 keV line, the 795 keV line in ^{134}Cs and the 1275 keV line in ^{154}Eu summed over all 25 nodes for each assembly. Numerical results for all assemblies are given in table 5.1.

A number of alternative approaches of the summing procedure were tried. For instance, there are reasons to omit the end parts of the assemblies in the summing procedure since the core physics calculations for these parts are expected to be less accurate than for the central part, see also fig 3.6. One may also try to use higher energy transitions in ^{134}Cs in order to bring down the influence of possible radial gradients the BU or to use lower energy transitions in ^{154}Eu in order to obtain a self-absorption effect similar to that of the radiation from the other nuclei. However, no significant improvements over the approach taken here could be observed.

In sections 5.2 and 5.3 data are presented in two ways. In section 5.2 the intensities for each isotope have been fitted to eq. (2.1) (^{137}Cs) or eq. (2.2) (^{137}Cs and ^{154}Eu). Before the fit the intensities have been corrected for CT using the operator's declared values. In this procedure, which essentially is a calibration, the slope coefficient K_x and the exponent κ have been determined for each isotope. The evaluation has been made separately for each campaign as well as for the complete data set.

In section 5.3 results are presented from a simultaneous determination of BU and CT by using intensities of two isotopes according to equations (2.3) and (2.4). Here the calibration constants K_x and κ for each isotope from section 5.2 have been used.

Reactor	Ass. #	BU (GWd/tU)	CT (days)	Enrich. (%)	No. of cycles	α (^{137}Cs)	α (^{134}Cs)	α (^{154}Eu)	Norm. factor	Int. ^{137}Cs (cps)	Int. ^{134}Cs (cps)	Int. ^{154}Eu (cps)
Camp. F												
F2	12961	36.05	683	3.03	5	1.0589	1.4373	1.1094	1.4106	875.98	1272.36	102.97
F2	5536	14.84	2866	2.09	3	1.0448	1.3188	1.0803	1.4106	313.15	33.85	14.11
F2	12921	36.1	683	3.03	5	1.0635	1.5506	1.1310	1.4106	868.93	1155.28	101.56
F2	12922	36.1	683	3.03	5	1.0635	1.5506	1.1310	1.4106	863.29	1141.18	100.15
F2	8897	29.15	1768	2.82	4	1.0452	1.2698	1.0703	1.4106	655.93	355.47	62.07
F2	12935	34.33	264	3.03	6	1.0880	1.9259	1.2097	1.4106	836.49	1173.62	90.28
F2	8921	29.83	957	2.82	6	1.0827	1.7750	1.1796	1.4106	674.27	500.76	59.25
F2	11463	29.97	684	2.93	5	1.0669	1.6239	1.1454	1.4106	706.71	706.71	66.30
F2	12929	33.07	958	3.03	4	1.0501	1.3428	1.0872	1.4106	808.27	854.82	84.64
F2	12957	33.88	958	3.03	4	1.0502	1.3444	1.0875	1.4106	832.25	938.05	93.10
Camp. G												
B1	9330	41.1	1511	2.92	5	1.0618	1.4271	1.1106	0.7981	1001.62	775.75	95.77
B1	9329	41.1	1511	2.92	5	1.0618	1.4271	1.1106	0.7981	996.03	765.38	95.77
B1	9313	35.3	1516	2.92	4	1.0458	1.2629	1.0686	0.7981	872.32	624.91	79.81
B1	10290	32	1516	2.95	4	1.0458	1.2629	1.0686	0.7981	774.96	541.91	68.64
B1	10287	33.1	1516	2.95	4	1.0458	1.2629	1.0686	0.7981	805.28	574.63	72.63
B1	10286	32.6	1516	2.95	4	1.0458	1.2629	1.0686	0.7981	794.11	557.87	71.03
R1	5769	32.6	1903	2.75	7	1.0951	1.9138	1.2139	0.7981	726.27	259.38	58.26
F2	8962	32.4	1583	2.81	4	1.0474	1.3025	1.0781	0.7981	811.67	534.73	69.43
F2	8960	29.5	1583	2.81	4	1.0474	1.3025	1.0781	0.7981	706.32	421.40	57.46
F2	5535	19.9	1584	2.09	6	1.1148	2.1965	1.2762	0.7981	430.18	106.95	24.74
Camp. I												
F2	12950	37.9	1277	3.05	5	1.0600	1.4575	1.1140	1.0000	901.00	806.00	91.00
F2	12952	33.2	857	3.05	6	1.0828	1.7976	1.1843	1.0000	797.00	703.00	70.00
F2	12961	36	1277	3.05	5	1.0589	1.4373	1.1094	1.0000	876.00	758.00	84.00
F2	9500	33.3	1953	2.84	5	1.0599	1.4002	1.1043	1.0000	779.00	369.00	67.00
F2	9501	30	1953	2.84	5	1.0559	1.3273	1.0882	1.0000	686.00	308.00	57.00
F2	9502	31.5	1953	2.84	5	1.0658	1.5973	1.1387	1.0000	721.00	270.00	53.00
F2	9504	31.1	1953	2.84	5	1.0719	1.7153	1.1630	1.0000	708.00	235.00	49.00
F2	9508	31.3	1953	2.84	5	1.0680	1.6242	1.1450	1.0000	711.00	259.00	53.00
F2	9510	32.1	1953	2.84	5	1.0677	1.6257	1.1450	1.0000	733.00	271.00	55.00
F2	9515	32.6	1954	2.84	5	1.0663	1.5815	1.1375	1.0000	744.00	294.00	58.00
F2	9521	29.3	1954	2.84	5	1.0668	1.5943	1.1397	1.0000	664.00	226.00	46.00
F2	9525	29.5	1954	2.84	5	1.0644	1.5568	1.1315	1.0000	687.00	247.00	49.00
F2	9529	33.6	1954	2.84	5	1.0662	1.5639	1.1352	1.0000	765.00	306.00	57.00
B1	9282	33.1	1888	2.91	5	1.0659	1.6107	1.1411	1.0000	781.00	307.00	57.00
F2	9512	35.2	1953	2.84	5	1.0578	1.3938	1.1007	1.0000	822.00	411.00	71.00
B1	9285	33	1888	2.91	5	1.0697	1.7144	1.1590	1.0000	781.00	294.00	56.00
B1	9287	34.2	1888	2.91	5	1.0693	1.6496	1.1505	1.0000	798.00	315.00	60.00
B1	9288	31.4	2331	2.91	4	1.0466	1.3086	1.0787	1.0000	722.00	245.00	57.00
B1	9291	32.5	2332	2.91	4	1.0478	1.3256	1.0828	1.0000	769.00	265.00	62.00
B1	9292	32.1	2332	2.91	4	1.0468	1.3003	1.0776	1.0000	763.00	270.00	62.00
B1	9295	35.9	1889	2.91	5	1.0690	1.6253	1.1473	1.0000	837.00	347.00	64.00
B1	9297	34	1889	2.91	5	1.0692	1.6460	1.1497	1.0000	819.00	323.00	58.00
B1	9302	35.6	1889	2.91	5	1.0687	1.6376	1.1486	1.0000	827.00	340.00	63.00
B1	10287	33.1	1889	2.95	4	1.0458	1.2629	1.0686	1.0000	790.00	412.00	67.00

Table 5.1. Declared data for the fuel assemblies considered in this work together with measured gamma-ray intensities, normalised to campaign I and correction factors for power history. The measured gamma-ray intensities are not corrcted for cooling time nor power history.

5.2 Determination of the calibration constants K_x and κ

5.2.1 ^{137}Cs

For each assembly measured a data point (I,β) was defined with

$$I = I_1 \alpha_1 e^{\lambda_1 CT} \qquad \text{(Eq. 5.1)}$$

Here I_1 is the measured gamma-ray intensity of the ^{137}Cs line and CT is the operators' declared value. The correction factor α_1 is calculated using eq. (2.10) and the operators' declared data. For each campaign a straight line

$$I = K_1 \beta \qquad \text{(Eq. 5.2)}$$

was fitted to the data points. Figure 5.1 shows an example of such a fit.

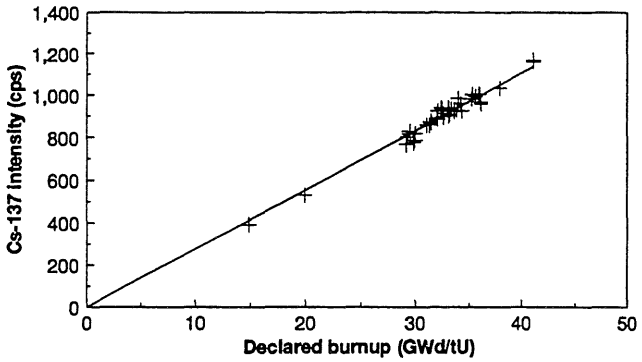

Figure 5.1. Measured intensities from ^{137}Cs, corrected for cooling time and power history, v. s. burnup. The line is a least squares fit to the data.

The slope coefficient K_1 with standard deviation (S. D.) and the S. D. for the individual points are given for the three campaigns and the summed data in table 5.2. One may first observe that the values of K_1 obtained in the three campaigns agree well enough to suggest that the three sets of data can be added for a common fit, which yields an S. D. of the individual points of 2.7%. This value is of interest since it directly gives the relative uncertainty of the BU as measured with the HRGS method.

The magnitude of this uncertainty is influenced by a number of effects or circumstances which will be discussed in the following:

1. Counting statistics. Typically 10^5-10^6 counts have been collected for the ^{137}Cs peak, implying a contribution in the range 0.1-0.3% to the error.
2. Systematic experimental errors. A number of possible sources of systematic errors have been investigated, refs. /6,10/. The errors that may influence the results given in table 5.2 are all estimated to be less than 1%.
   To check the reproducibility of the measurements all fuel assemblies studied in campaign F were measured twice. The average difference between the two measurements was 0.6%. Another indication on the degree of reliability of the measurements is obtained from the measurements of fuel assemblies with symmetric positions in the core, which are expected to have identical values of BU. Three such pairs have been measured and show pairwise an agreement within 1% of the gamma intensity.
3. Uncertainty in the declared BU. The accuracy of the BU values obtained in the core physics calculations is not very well known. Rather large uncertainties are known to exist for the parts of the fuel subject to large void coefficients (cf. fig 3.6), and some uncertainty is also expected in the earliest power cycles of the fuel. At the end of the fuel cycle, however, these uncertainties can be assumed to level out and the declared BU values generally seem to be believed by the core

physicists to be accurate within 2-5%. One may observe that this estimate agrees well with the S. D. values given in table 5.2. This line also shows that the S. D. value obtained for each campaign is somewhat smaller than that obtained for the complete set of data. This is even more clear if data for a particular reactor are singled out. One such case is shown in the table, for Forsmark 2, which also shows a significantly (~ 4%) smaller value of the slope coefficient K_1 than the campaigns performed at CLAB. It may in this case be questioned whether the fact that the measurements were performed at different sites may introduce any systematic errors. This is not likely here since the Forsmark data were normalised to those at CLAB by measuring the same fuel assembly at both places, thereby eliminating the possible sources of error that could be associated with the use of the reference source. Similar results of small (a few percent) but significant deviations between slope coefficients for fuel from different reactors measured in the same campaign have been obtained in the CLAB measurements.

The S. D. of the slope coefficient K_1 depends somewhat on the homogeneity of the data set. For example, in campaign F there were three assemblies measured which had a low BU and an extraordinary irradiation history. They originate from the initial core of the F2 reactor and was in operation during three and seven cycles with a final burnup of 21.8 and 22.6 GWd/tU, respectively. The K_1 value obtained with these assemblies included in the analysis for campaign F is 26.58±0.18. Also the S. D. of the ^{137}Cs data points increase from 1.72% to 2.98%.

4. Possible fundamental uncertainties of the method
   As discussed in section 2.5 the gradient of the BU in BWR fuel assemblies in combination with the self absorption of gamma-rays in the fuel assembly may give rise to systematic effects. From calculations they are estimated to be of the order of ±1% in the BU range 20-40 GWd/tU. An other possible source of error would be a varying degree of radial redistribution of the Caesium within the fuel pins. However, assuming a maximal axially symmetric redistribution within each fuel pin, this would affect the measured intensities less than 5%.

The lower part of table 5.2 is based on the same data as the upper part with the difference that the data have not been corrected for power history. For the slope coefficient of the ^{137}Cs intensity it is seen that neglecting the power history correction does not impair the results significantly. This is expected in view of the long half-life of ^{137}Cs.

5.2.2 ^{134}Cs and ^{154}Eu

In analogy with the procedure described in section 5.2.1, a data point (I,β) was calculated from

$$I = I_2 \alpha_2 e^{\lambda_2 CT} \qquad \text{(Eq. 5.3)}$$

where I_2 is the experimentally observed count rate on the 795 keV and 1275 keV transitions in ^{134}Cs and ^{154}Eu, respectively, CT is the operator's declared CT and α_2 is the correction factor for power history as calculated from eq. (2.9). A fit of the data points from all campaigns to the exponential of eq. (2.2) is shown in figs. 5.2 and 5.3. The fitting parameters K_2 and κ from this fit and for the fits of each campaign are given in table 5.2. As expected the parameter κ is found to be close to 2 for ^{134}Cs, while for ^{154}Eu a lower value is found.

The parameters fitted agree well within the errors for the different campaigns but the variation of K_2 is sometimes rather large, up to 50% ,which is much more than might be expected from the variation in the data points. This is due to the rather strong coupling of the two fitting parameters, which lead to a good fit of the data for a rather large variety of combinations of the parameters.

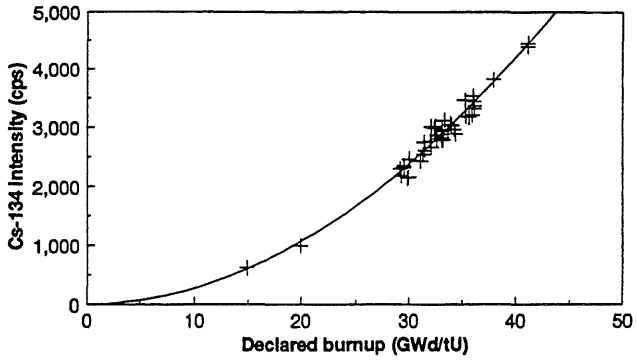

Figure 5.2. Measured intensities from ^{134}Cs corrected for cooling time, power history and initial enrichment v. s. burnup. The curve is a least squares fit to the data.

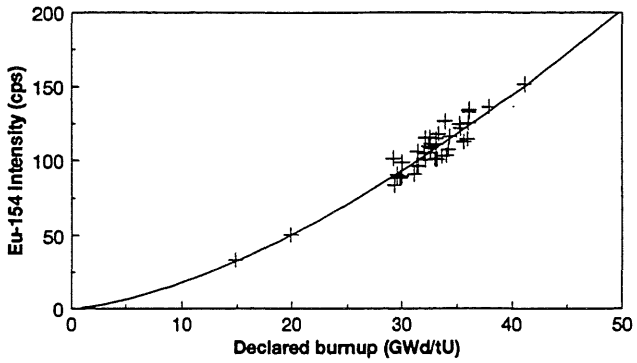

Figure 5.3. Same as in fig. 5.2 but for ^{154}Eu.

The relative S. D. of the individual points is larger than for ^{137}Cs by a factor of 1.7 for ^{134}Cs and a factor of 2.2 for ^{154}Eu. It has not been possible within the economic limits of this work to deduce the reason for this, but besides the list of sources of errors given in section 5.2.1 some additional error sources may be mentioned:

Uncertainty in the correction for power history. The half-lives for ^{134}Cs and ^{154}Eu are both comparable or shorter than the fuel cycle, which makes the correction for power history much more important than for ^{137}Cs. This can be inferred from the lower part of table 5.2, which shows the values of the coefficients obtained from data points that have not been corrected for power history. One observes that the values for ^{134}Cs and ^{154}Eu given in this part of the table have much larger uncertainties and vary much more relative to the parameters based on the corrected data than do the values for ^{137}Cs. In performing the correction, from power history, eq. (2.9), only corrections down to a time scale of one whole power cycle were considered. It is likely, especially for ^{134}Cs, that one would obtain a smaller S. D. of the fit if the power history could be corrected for in more detail.

Another possible source of error is that in the correction function, eq. (2.14), for practical reasons, the time-dependence of the activity during irradiation was not given its exact form but approximated with a simpler function. Calculations performed with different functions showed however that this part of the correction was not important for the fit.

Uncertainty in the form of the fitted function. The data points of ^{154}Eu in general give a fit with a S. D. of more than a factor 2 larger than that obtained for the corresponding data for ^{134}Cs. The main reason for this is not clear, but it should be observed that while the function fitted to the ^{134}Cs points theoretically should be very close to a quadratic function, the function fitted to the ^{154}Eu data is only a first approximation of a more complex function, that may vary between different positions in the core and different axial positions in the assembly.

The possibility to improve the fit by using data from only a limited axial part of the assemblies was investigated. For all three isotopes the evaluation of the data and the fit to eqs. (2.1) and (2.2) were

repeated using only the intensities measured between the nodes #9-17. No improvement of the fits were observed.

Influence of original enrichment. The influence of the enrichment on the intensities measured have only been treated approximately for these isotopes, see section 2. It is possible that a more accurate treatment could lead to a better fit of the data.

5.3 Simultaneous determination of BU and CT

Provided that the corresponding calibration parameters K_x and κ are known, eqs. (2.3 and (2.4) can be used to determine BU and CT from measured intensities of two isotopes, i. e. ^{137}Cs and ^{134}Cs or ^{137}Cs and ^{154}Eu. The results of such calculations are demonstrated in the following under two different circumstances: (i) Information on power history is available. (ii) No information on the assembly is available. Case (i) corresponds to a procedure of verification of the fuel parameters, while case (ii) corresponds to an independent measurement of the parameters. The accuracy in case (ii) is however considerably worse than in case (i).

Data points corrected[1)]

Campaign	F	G	I	F+G+I
No. of ass.	10	10	24	44
K_1 (^{137}Cs)	26.73±0.14	28.12±0.16	27.92±0.10	27.71±0.11
S. D. (^{137}Cs) (%)	1.72	2.34	1.75	2.68
K_2 (^{134}Cs)	3.43±0.69	2.24±0.46	3.18±1.63	2.83±0.42
S. D. (^{134}Cs) (%)	4.45	3.37	4.39	4.47
κ (^{134}Cs)	1.91±0.06	2.05±0.06	1.95±0.15	1.98±0.04
K_2 (^{154}Eu)	0.48±0.13	0.54±0.05	0.57±0.41	0.55±0.11
S. D. (^{154}Eu) (%)	5.93	1.66	6.10	5.98
κ (^{154}Eu)	1.56±0.08	1.52±0.03	1.49±0.21	1.51±0.06

Data points not corrected

Campaign	F	G	I	F+G+I
No. of ass.	10	10	24	44
K_1 (^{137}Cs)	25.16±0.19	26.59±0.26	26.27±0.11	26.11±0.12
S. D. (^{137}Cs) (%)	2.45	4.54	2.16	3.43
K_2 (^{134}Cs)	4.50±3.43	0.23±0.24	2.52±4.13	1.56±0.86
S. D. (^{134}Cs) (%)	17.60	18.05	13.80	17.42
κ (^{134}Cs)	1.72±0.22	2.60±0.30	1.89±0.47	2.03±0.16
K_2 (^{154}Eu)	0.32±0.13	0.16±0.06	0.44±0.45	0.28±0.08
S. D. (^{154}Eu) (%)	9.21	6.20	8.63	8.89
κ (^{154}Eu)	1.65±0.12	1.84±0.11	1.53±0.29	1.67±0.08

1) The data points have been corrected for power history according to eqs. (2.10) and (2.14). Also a correction was made for initial enrichment in the cases of ^{134}Cs and ^{154}Eu. See text for further details.

Table 5.2. Results of the calibration procedure for each campaign and the grand total of all campaigns.

5.3.1 ^{134}Cs and ^{137}Cs

Fig 5.3.1a and b shows the agreement between the experimentally obtained BU and CT, respectively and the declared values for case (i). The corresponding diagrams for case (ii) is shown in fig 5.3.2a and b. Standard deviations for data sets are given in table 5.3.

As expected the S. D. of the BU in case (i) is about the same as that obtained for ^{137}Cs in the calibration fit, section 5.2.1. In this case the CT can be verified within two months.

In case (ii), the BU can still be obtained with about 3% S. D., while the uncertainty of the CT has increased to about 6 months. These numbers are in principle not sensitive to the duration of the CT up to about 20 years, when the decay of ^{134}Cs starts causing large statistical uncertainties.

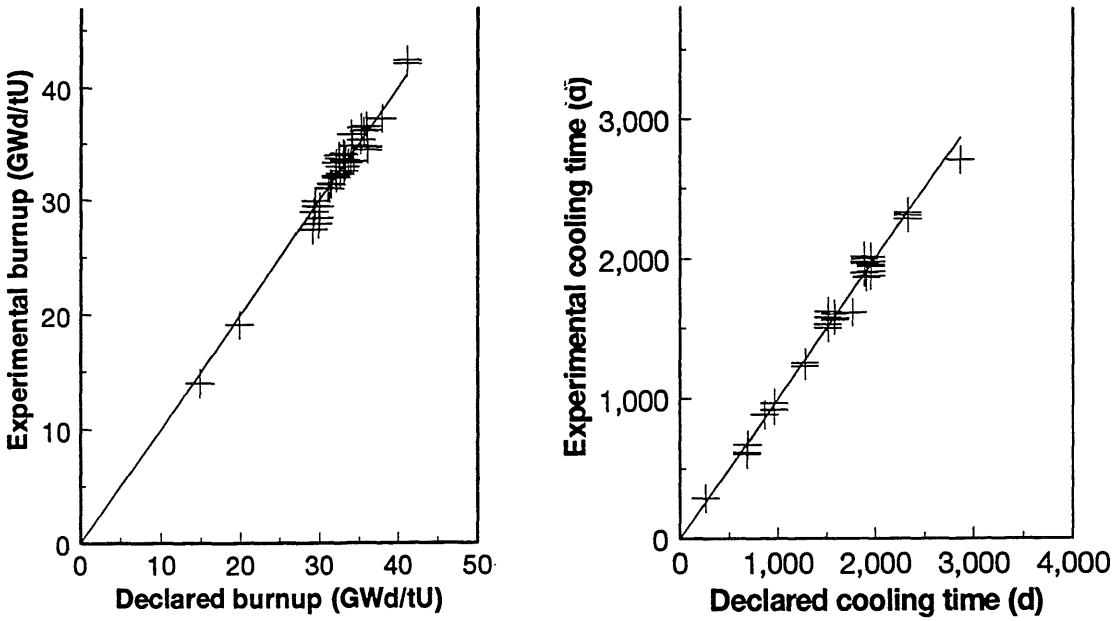

Figure 5.3.1. a) Experimentally obtained burnup v. s. declared burnup. b) Cooling time determined experimentally v. s. declared cooling time. In both cases the information on power history is available. The line in the figure corresponds to a least squares fit of the experimentally obtained values to the declared ones.

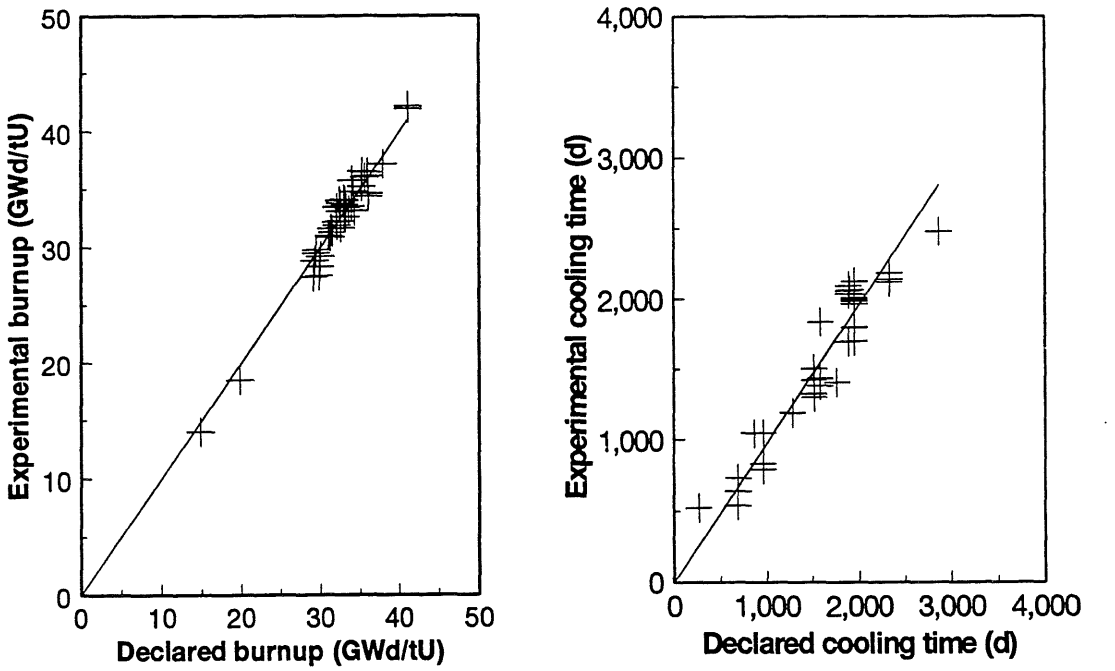

Figure 5.3.2. Same as in fig. 5.3.1 but for the case where no information on the power history is available.

5.3.2 ^{154}Eu and ^{137}Cs

Figs. 5.3.3 and 5.3.4 show the agreement of BU and CT for the combination ^{154}Eu + ^{137}Cs in analogy with figs. 5.3.1 and 5.3.2. The corresponding S. D. are given in table 5.3.

The numbers given for case (ii) imply that these data allow the measurement of BU with an accuracy of about 6%, while the CT cannot be determined within better than about 2 years. No significant improvement is observed for the corrected data.

It was noted in section 5.2 that the data for ^{154}Eu scatter more than for the other isotopes. The explanation for this can be found by differentiating eqs. (2.3) and (2.4) with respect to I_2 and re-arranging:

$$\frac{\Delta\beta}{\beta} = \frac{\Delta I_2}{I_2} \qquad \text{Eq. (5.4)}$$

and

$$\Delta CT = C\frac{\Delta I_2}{I_2} \qquad \text{Eq. (5.5)}$$

From eq. (5.4) we conclude that the relative uncertainty in β is equal to the relative uncertainty in the ^{134}Cs or ^{154}Eu intensities. It is inferred from table 5.3 that the relative uncertainty of the ^{154}Eu intensities is roughly a factor of 2 larger than for the ^{134}Cs -intensities.

The uncertainty in CT, eq. (5.5), is largely dependent on the constant factor C which, in turn, is dependent on the specific values of the decay constants. For ^{154}Eu C=7796 days and for ^{134}Cs C=1253 days i. e. a factor of 6 smaller in this case.

We conclude that the uncertainties discussed above implies that the total uncertainty in CT for the combination of ^{137}Cs +^{154}Eu is a factor of 12 larger than for the corresponding value for ^{137}Cs +^{134}Cs. This result is supported by the results given in table 5.2.

5.4 Determination of CT from the ratio ^{154}Eu/^{134}Cs

As pointed out in section 2.4, an alternative way of obtaining CT independently is to use eq. (2.5). In figure 5.4 we show a plot where the ratio between the uncorrected intensities of ^{154}Eu /^{134}Cs are plotted v. s. cooling time. The curve in fig. 5.4 is a least squares fit of the form:

$$R = Ae^{-CT(\lambda_2-\lambda_3)} \qquad \text{Eq. (5.6)}$$

Where λ_2 and λ_3 corresponds to the decay constants for ^{154}Eu and ^{134}Cs, respectively and A is a fitting parameter. The S. D. of the ratio corresponds to a S. D. in cooling time of 170 days.

This method of determining cooling time can be used up to about 20 years of cooling time due to the same arguments as discussed in section 2.4.

Data points corrected[1)]

Campaign	F	G	I	F+G+I
No. of ass.	10	10	24	44
Δβ (^{137}Cs) (%)	1.72	2.34	1.75	2.68
Δβ (^{134}Cs) (%)	1.87	2.63	1.92	2.93
Δβ (^{154}Eu) (%)	3.14	3.91	3.79	5.56
ΔCT (^{134}Cs) (d)	58	61	56	62
ΔCT (^{154}Eu) (d)	416	278	477	565

Data points not corrected

Campaign	F	G	I	F+G+I
No. of ass.	10	10	24	44
Δβ (^{137}Cs) (%)	1.88	4.37	2.06	3.20
Δβ (^{154}Eu) (%)	2.90	6.82	3.81	6.21
ΔCT (^{134}Cs) (d)	167	179	152	170
ΔCT (^{154}Eu) (d)	514	560	564	698

1) The data points have been corrected in the same way as in table 5.2.

Table 5.3. Results of the burnup and cooling time verifications. The upper part corresponds to data corrected for power history and initial enrichment. The lower part corresponds to a situation where no declared parameters are available.

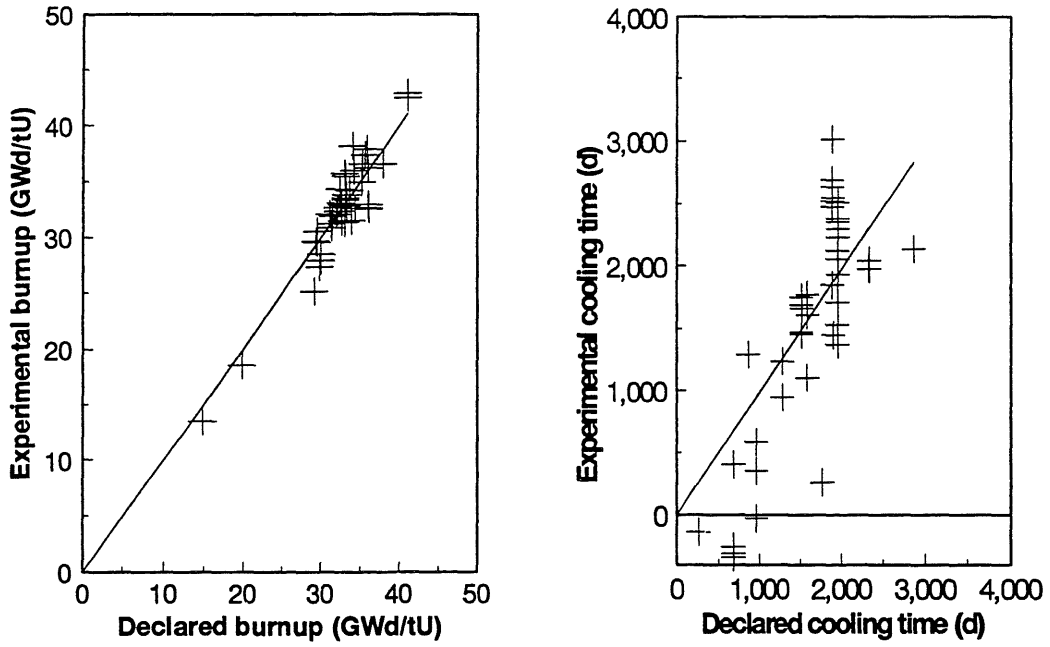

Figure 5.3.3. The analogue figure to 5.3.1 but referring to the combination ^{137}Cs + ^{154}Eu.

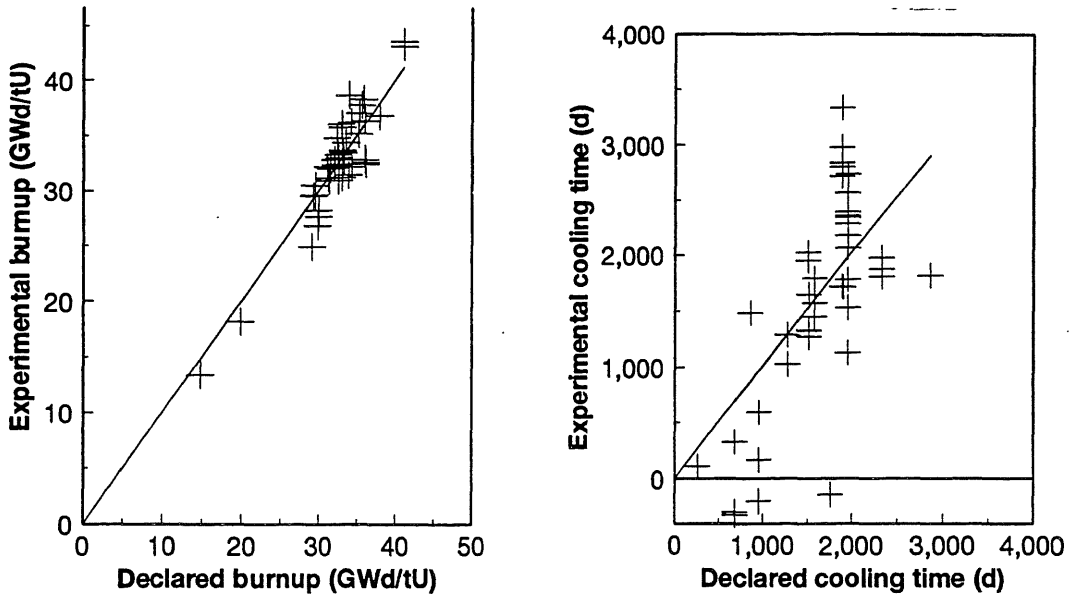

Figure 5.3.4. Same as in fig. 5.3.3 but for the case where no information on the power history is available.

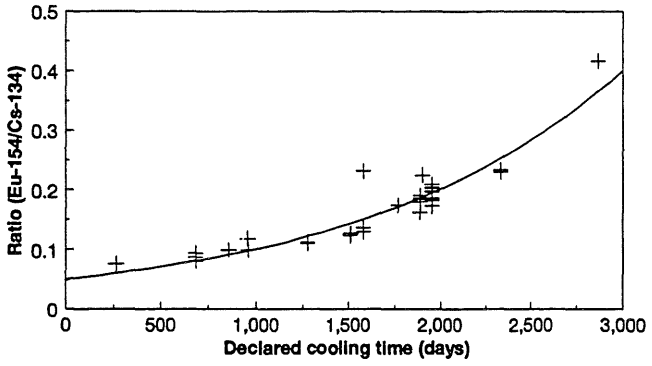

Figure 5.4. Plot showing the ratio ^{154}Eu / ^{134}Cs v. s. declared cooling time. The curve is a least squares fit and the corresponding S. D. of the data points is 170 days.

6 Discussion

The results presented in section 5 form a basis of a discussion of the practicability of the HRGS method for safeguard induced measurements on BWR fuel. It may be stated in general that, provided the proper equipment is installed, the HRGS method is both fast and accurate. Typical measurement times are 15 min per assembly. An estimation gives that for fuel up to about 20 years of age, burnup and cooling time can be verified at a level of 2-3% S. D. and a few months, respectively. For older fuel, with up to about 50 years cooling time, the latter can be verified at a level of accuracy of about 1.5 years S. D.

The present experiments have utilised existing elevator and collimator installations. This is however no necessary requirement, similar measurements have been made using a fuel handling machine instead of an elevator and a transportable underwater installation including a collimator and a Ge detector /11/.

In section 2.1 five fuel parameters were listed of which three have been treated extensively in this report. One of the remaining two parameters, the initial enrichment of the fuel, has only been studied theoretically, since essentially all assemblies measured here has very nearly the same average enrichment. It remains to verify experimentally the calculations reported in section 2.

The remaining fuel parameter listed, i. e. the integrity of the fuel assembly, has been of importance in the present study in the respect that a number of reconstructed fuel assemblies were admixed into our sets of standard assemblies. In general slightly lower K_1 values were observed for these assemblies, but the data are too scarce to allow a thorough evaluation.

The possibility to detect missing fuel pins has been considered at an initial stage in that some preliminary calculations have been made. Further calculations and experiments have to be conducted in order to appreciate the sensitivity of the HRGS data as regards this effect.

7 Acknowledgements

This project was initiated and economically supported by SKI. Discussions with Lars Hildingsson and Göran af Ekenstam are gratefully acknowledged. Also the staffs at CLAB and at the different power plants, both in Sweden and Finland where some of the measurements were performed, are acknowledged.

8 References

[1] D. D. Cobb et al., Non-destructive verification and assay systems for spent fuel, Los Alamos Report LA-9041, vol. II (1982) and references therein.

[2] G. af Ekenstam and M. Tarvainen, Independent burnup verification of BWR type nuclear fuel by means of the ^{137}Cs activity, STUK-A52 (1987)

[3] R. Berndt, Verification of spent PWR fuel data using the ^{154}Eu, ^{134}Cs and ^{137}Cs activities, Kernenergie 31 (1988) 58.

[4] H. Graber, G. Hofmann and R. Berndt, Correlations of burnup with concentration ratios for irradiated LWR fuel, IAEA-SM-260.

[5] A. Bäcklin, A. Håkansson, P. Björkholm and A. Dyring, A gamma-ray spectroscopy system for burnup measurements of nuclear fuel, Proc. 13th ESARDA Ann. Symp. Avignon 1991.

[6] M. Tarvainen, A. Bäcklin and A. Håkansson, Calibration of the TVO spent BWR reference fuel assembly, STUK-YTO-TR37, Finnish Centre For Radiation Research, Helsinki (1992).

[7] A. Bäcklin, A. Håkansson and L. Hildingsson, Gamma Scanning At High Count Rates Of Irradiated BWR Fuel For Safeguard Purposes, Proc. 34th Ann. Meeting of the Institute of Nuclear Materials Management, Scottsdale Arizona July 18-21 1993.

[8] A. Håkansson, A. Bäcklin, L. Hildingsson and G. af Ekenstam, High Resolution Gamma-Ray Spectroscopy Measurements of Spent Fuel, IAEA-SM-333/87 (1994).

[9] I. Matsson, ORIGEN 2 Simulations of Spent BWR Fuel with Different Burnup, Power History and Initial Enrichment, project work in applied nuclear physics (1995).

[10] P. Björkholm, A. Dyring, A Study of a High Count Rate Gamma Spectrometer System for Burnup Measurements, UPTEC 90015E, Institute of Technology, Uppsala University (1990).

[11] B. Grapengiesser, ABB-Atom, Private communication.

Postadress/Postal address

SKI
S-106 58 STOCKHOLM

Telefon/Telephone

Nat 08-698 84 00
Int +46 8 698 84 00

Telefax

Nat 08-661 90 86
Int +46 8 661 90 86

Telex

11961 SWEATOM S